RSC Advances

PAPER

View Article Online
View Journal | View Issue

Cite this: *RSC Adv.*, 2021, **11**, 10203

Carbazole sulfonamide-based macrocyclic receptors capable of selective complexation of fluoride ion†

Na Luo,[a] Junhong Li,[a] Tao Sun,[b] Suran Wan,[a] Peijia Li,[a] Nan Wu,[a] Ya Yan[a] and Xiaoping Bao *[a]

Received 17th February 2021
Accepted 2nd March 2021

DOI: 10.1039/d1ra01285a

rsc.li/rsc-advances

Two carbazole sulfonamide-based macrocycles **1** and **2** were facilely synthesized and carefully evaluated for their anion recognition properties. The obtained results revealed that macrocycle **1** with a 1,3-xylyl linker was able to bind fluoride ion more strongly and selectively in acetonitrile medium than its strong competitors (like acetate and dihydrogen phosphate anions), with a large binding constant (K_a) of 50 878 M^{-1}. More importantly, an exclusive fluoride recognition was achieved for macrocycle **1** in the more polar DMSO-d_6 solution, albeit with a moderate affinity of K_a = 147 M^{-1}. Compared with macrocycle **1**, macrocycle **2** bearing a 2,6-lutidinyl linkage exhibited a remarkable change not only in the anion affinity but also in the anion selectivity, although with only a slight difference in their molecular structures.

Introduction

Fluoride ions play crucial roles in many chemical, biological, and environmental processes, thus the development of fluoride-selective receptors and/or sensors has become a research focus in the field of supramolecular chemistry.[1,2] However, only a handful of examples of anion receptors enabling the simultaneous discrimination of fluoride from its strong competitors (like acetate and dihydrogen phosphate anions) by means of their remarkably different affinities have been reported so far,[3–12] if ruling out some reports of specific reactions-based detection of fluoride. As we all know, the backbone of carbazole is an ideal platform for constructing efficient anion receptors since it is easy to install various anion binding groups onto this backbone and then cooperatively bind anions with the assistance of the 9-position NH unit.[13] Moreover, it has been shown that macrocyclic anion receptors are capable of pre-organizing relevant recognition sites, thus being favorable for achieving strong and selective complexation towards specific anions based on size and/or shape complementarity to the macrocycles.[14,15] Nonetheless, the preparation of such macrocycles generally requires lengthy and tedious synthetic procedures due to their sophisticated structures. Among the commonly-used anion-binding groups, sulfonamide NH can form a stronger N–H···anion hydrogen bond than its amide NH analogue.[16,17] In addition, the utilization of aromatic CH group as hydrogen-bond donor for constructing anion receptors was hitherto less studied,[18,19] although they had some unique advantages over the conventional NH/OH hydrogen-bond donors including a remarkable resistance towards the deprotonation event[20] and a larger affinity towards softer anions in some cases.[21] In 2016, we synthesized 1,8-disulfonamidocarbazole-dipyrromethane Schiff-base macrocycle & its reduced derivative and evaluated their anion binding properties by UV-vis and ^{1}H NMR titration methods.[22] The results indicated that two macrocyclic receptors exhibited strong binding interactions ($K_a > 10^4$ M^{-1}) with fluoride, acetate and dihydrogen phosphate ions over other anions in the highly competitive DMSO medium, but both macrocycles were poorly selective among these three anions.

Based on all of the above considerations, we herein reported a carbazole sulfonamide-based macrocycle **1** containing four hydrogen-bond donors as anion-binding sites, namely one carbazole NH, two sulfonamide NHs and one aromatic CH groups. In order to clarify the effects of aromatic CH group of the 1,3-xylyl linker in **1** on the anion-recognition behaviors, macrocycle **2** with a 2,6-lutidinyl linker was also synthesized for comparison.

Results and discussion

Preparation of macrocycles 1 and 2

As shown in Scheme 1, macrocycles **1** and **2** were facilely synthesized by condensation of carbazole-1,8-disulfonyl chloride **3** [22,23] with the appropriate diamines in dry CH_2Cl_2 using

[a]*State Key Laboratory Breeding Base of Green Pesticide and Agricultural Bioengineering, Key Laboratory of Green Pesticide and Agricultural Bioengineering, Ministry of Education, Center for Research and Development of Fine Chemicals, Guizhou University, Guiyang 550025, China. E-mail: baoxp_1980@aliyun.com*

[b]*College of Chemistry and Chemical Engineering, Guizhou Key Laboratory of High Performance Computational Chemistry, Guizhou University, Guiyang 550025, China*

† Electronic supplementary information (ESI) available: Crystallographic data of **1**, **2** & the complex $(\mathbf{1})_2 \cdot F^-$, ^{1}H NMR titration spectra, UV-vis titration spectra as well as ^{1}H NMR, ^{13}C NMR & HRMS spectral files of macrocycles **1** and **2**. CCDC 1976672, 2021529 and 1976667. For ESI and crystallographic data in CIF or other electronic format see DOI: 10.1039/d1ra01285a

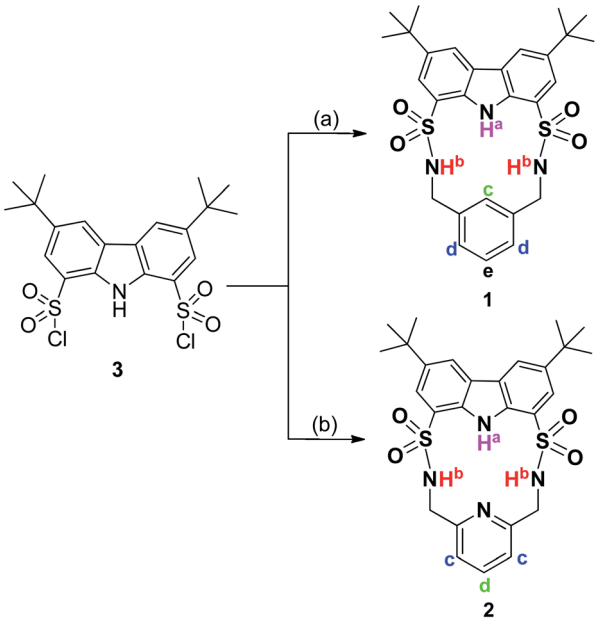

Scheme 1 Synthesis of macrocycles **1** and **2**. Reaction conditions: (a) 1,3-xylenediamine/dry CH_2Cl_2/dry TEA/rt/30%; (b) 2,6-lutidinylenediamine/dry CH_2Cl_2/dry TEA/rt/25%.

TEA as a catalyst, giving reasonable yields of 30% and 25%, respectively. Both macrocycles were fully characterized by ^{1}H NMR, ^{13}C NMR, and HRMS (high resolution mass spectrometry) techniques. Additionally, single crystals of **1** and **2** suitable for X-ray diffraction analysis were obtained by slow evaporation of their CH_3CN solution at room temperature. As shown in Fig. 1, two macrocycles both adopted a folded conformation in the solid state. More specifically, two sulfonamide NH protons in **1** pointed away from the macrocyclic cavity and the dihedral angle between carbazole plane and phenyl ring was measured to be 12.49°. In other words, NH and CH recognition units of **1** displayed a divergent orientation in the anion-free state. Unlike **1**, carbazole NH and one of the two sulfonamide NHs of **2** pointed in the same direction. Relative to **1**, the dihedral angle between two aromatic rings of **2** was slightly reduced to 11.20°.

Anion recognition studies

The binding interactions between macrocyclic receptors and a variety of anions (including spherical F^-/Cl^-/Br^-, tetrahedral $H_2PO_4^-$/HSO_4^-/ClO_4^-, and trigonal planar $PhCOO^-$/CH_3COO^-/NO_3^-) were initially investigated by ^{1}H NMR titration method in CD_3CN. Upon addition of tetra-*n*-butylammonium fluoride (TBAF) into a CD_3CN solution of **1** (Fig. 2a), the proton signals assigned to carbazole NH (H^a) and sulfonamide NHs (H^b) rapidly vanished and then reappeared (after 1.0 equiv. of F^-). Notably, remarkable downfield shifts were observed for these two signals throughout the whole titration process (+4.56 and +4.99 ppm, respectively), indicative of the formation of strong intermolecular hydrogen bonds between these NH protons and the bound F^-. As expected, the signal of aromatic CH (H^c) also underwent a relatively small but well-defined downfield shift of +0.58 ppm, proving its effective participation in the stabilization of the resultant $\mathbf{1}\cdot F^-$ complex. Both molar ratio (Fig. 2b) and Job's plot (Fig. S1†) methods provided vigorous supports for the formation of 1 : 1 $\mathbf{1}/F^-$ complex in CD_3CN solution. However, the binding interaction of **1** with F^- in this medium was too strong to be accurately determined by ^{1}H NMR titration method (K_a > 10 000 M^{-1}), as inferred from the presence of a sharp titration isotherm in Fig. 2b.[24,25]

Unlike fluoride, the signal of carbazole NH in **1** was found to be traceable during the overall titration process and move downfield consistently (from 9.14 to 9.84 ppm) after addition of $H_2PO_4^-$ (Fig. 3a). Likewise, the signal of H^c also underwent a clear downfield shift from 7.14 to 7.49 ppm. Notably, a strong binding with $H_2PO_4^-$ by macrocycle **1** (K_a = 4920 M^{-1}) was observed in acetonitrile (Fig. 3b).

After addition of other competitive anions like $PhCOO^-$ and CH_3COO^- (Fig. S2 and S4†), two NH signals of **1** disappeared rapidly. Meanwhile, the signal of H^c experienced a continuous downfield shift of *ca.* +0.78 and +0.44 ppm, respectively. In the case of chloride ion (Fig. S6†), sulfonamide NH of **1** exhibited a pronounced downfield shift of +0.61 ppm. At the same time,

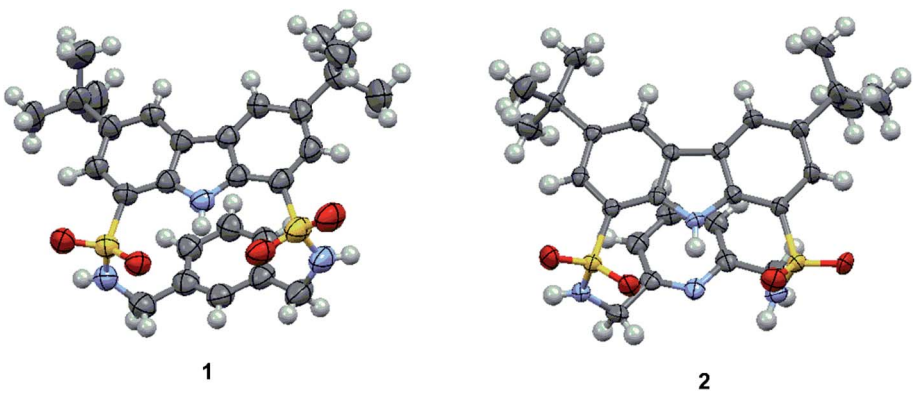

Fig. 1 Crystal structures of macrocycles **1** and **2**.

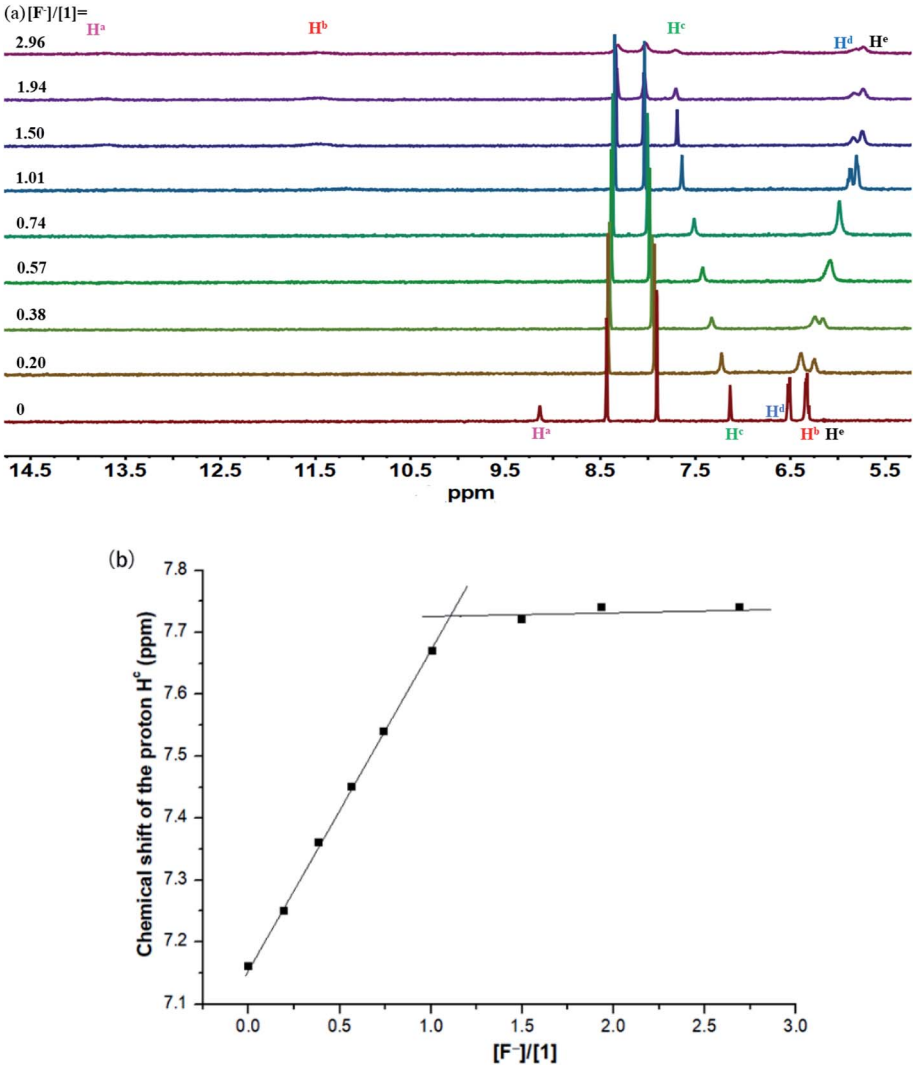

Fig. 2 (a) Stack plot of ^{1}H NMR titration of macrocycle **1** (1.6 mM) with TBAF in CD_3CN at 298 K. (b) Chemical shift changes of the proton H^c in **1** upon addition of TBAF in CD_3CN (K_a > 10 000 M^{-1}).

a small downfield shift of +0.26 ppm was also observed for aromatic CH. In contrast, carbazole NH only underwent a slight downfield shift of +0.05 ppm during the titration process. These findings clearly indicated that chloride ion was bound mainly by three intermolecular hydrogen bonds, contributing from two SO_2NH and one CH units.

In all cases except for fluoride ion, the ^{1}H NMR titration profiles gave the best fitting results using a 1 : 1 binding model (Table 1). For macrocycle **1**, the observed binding trend followed the order F^- (>10 000 M^{-1}) > $H_2PO_4^-$ (4920 M^{-1}) > $PhCOO^-$ (1013 M^{-1}) > CH_3COO^- (279 M^{-1}) > Cl^- (91 M^{-1}) > Br^- (24 M^{-1}) > NO_3^-/HSO_4^- (<10 M^{-1}) > ClO_4^- (no binding), which was inconsistent with the Hofmeister order of related anions ($H_2PO_4^-$ > CH_3COO^- > F^- > Cl^- > Br^-).[26] Of note, an unusual preference of **1** for tetrahedral $H_2PO_4^-$ over more basic & trigonal planar $PhCOO^-$ and CH_3COO^- was seen. The same binding trend was also found for macrocycle **2**, with the exception of a reversed order involving HSO_4^- and Br^-. It was noteworthy that two types of protons on the pyridine ring of **2** (H^c and H^d) both experienced a visible upfield shift upon exposure to F^-, $H_2PO_4^-$, CH_3COO^-, $PhCOO^-$, and Cl^- ions (Fig. S22, S24, S26, S28, and S32†), which was presumably caused by the proximity effect between these anions and the pyridine moiety after the complexation.

To accurately quantify binding affinities of both macrocycles towards F^- in acetonitrile solution, UV-vis titration studies were subsequently carried out. As shown in Fig. 4, a gradual increase in the absorption peak at 294 nm was detected for **1**, in the presence of increasing concentrations of TBAF. Meanwhile, two pseudo-isosbestic points were discovered at 305 and 355 nm. A 1 : 1 **1**/F^- binding model generated an excellent fitting result with K_a = 50 878 M^{-1} (consistent with the affinity range determined by ^{1}H NMR titration experiments), which was at least ten times higher than its nearest competitor $H_2PO_4^-$. To validate the nature of fluoride-induced spectroscopic changes of **1** (intermolecular hydrogen-bonding interactions or NH

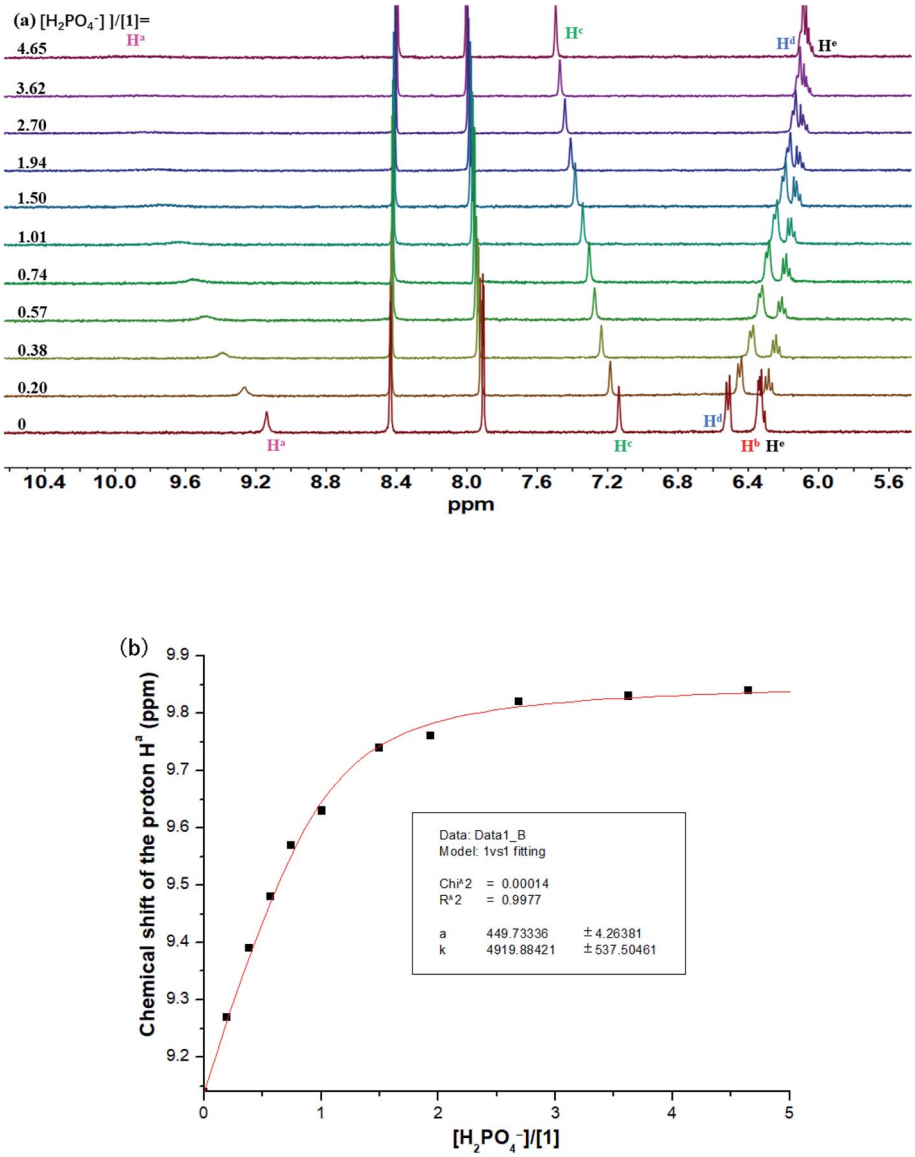

Fig. 3 (a) Stack plot of ^{1}H NMR titration of macrocycle **1** (1.6 mM) with $TBAH_2PO_4$ in CD_3CN at 298 K. (b) Fitting binding isotherms of macrocycle **1** with $TBAH_2PO_4$ in CD_3CN at 298 K, showing chemical shift changes of the proton H^a based on a 1 : 1 binding model.

deprotonation effect), the titration of **1** with strong base TBAOH was also performed. As shown in Fig. S38,† the absorption peak at 294 nm of **1** was considerably weakened upon addition of OH^-, along with a noticeable enhancement in the absorption bands centered at 275 and 325 nm. The above phenomena were completely different with those caused by F^-, which confirmed that multiple hydrogen-bonding interactions between **1** and fluoride accounted for the observed spectral changes in Fig. 4. In addition, the affinity of macrocycle **2** with F^- was determined to be 12 885 M^{-1} under the same experimental conditions (Fig. S39 and S40†).

After a close inspection of the data from Table 1, some preliminary conclusions could be drawn as follows: compared with **1**, a decrease in the affinity was detected for **2** with F^-, $H_2PO_4^-$, and Br^-, with a value of 3.9-, 2.0- and >2.4-fold, respectively. On the contrary, a higher affinity of **2** than **1** was discovered towards other anions like $PhCOO^-$, CH_3COO^-, Cl^-, and HSO_4^- (ranging from 2.0- to >4.2-fold). For macrocycle **1** bearing a 1,3-xylyl linker, the presence of an additional aromatic CH group as the potential anion-binding site was beneficial to anion complexation. After replacing the 1,3-xylyl linker with a 2,6-lutidinyl spacer, the resultant **2** was probably endowed with a certain degree of preorganization for its SO_2NH protons in solution (*via* intramolecular hydrogen-bonding interactions with the pyridine nitrogen atom), which was also conducive to anion binding. Simultaneously, this replacement meant the loss of an additional anion-binding site. Therefore, different change trends in the affinity towards various anions were observed for two macrocycles, depending on comprehensive outcomes of the aforementioned factors. Among all the tested

Table 1 Binding constants (K_a/M^{-1})[a] and selectivity factors for macrocycles **1** and **2** with various anions[b] in acetonitrile solution at 298 K

	1	**2**	K_a(**1**)/K_a(**2**)
F^-	50 878 ± 4721[c]	12 885 ± 1962[c]	3.9
$H_2PO_4^-$	4920 ± 538	2428 ± 309	2.0
$PhCOO^-$	1013 ± 91	2005 ± 75	0.5
CH_3COO^-	279 ± 21	940 ± 46	0.3
Cl^-	91 ± 2	335 ± 7	0.3
Br^-	24 ± 1	<10	>2.4
HSO_4^-	<10	42 ± 6	<0.2
NO_3^-	<10	<10	—
ClO_4^-	NB[d]	NB[d]	—
$K_a(F^-)/K_a(H_2PO_4^-)$	10.3	5.3	1.9
$K_a(F^-)/K_a(PhCOO^-)$	50.2	6.4	7.8
$K_a(F^-)/K_a(CH_3COO^-)$	182.4	13.7	13.3
$K_a(F^-)/K_a(Cl^-)$	559.1	38.6	14.5

[a] Determined by the ^{1}H NMR titration experiments in CD_3CN, by monitoring the proton signal of the receptors showing the most significant chemical shift changes over the titration process. The errors in the K_a values were within 15%. The R^2 values for the 1 : 1 non-linear fitting to determine K_a values ranged between 0.981 and 0.999. [b] All the anions were used as their tetrabutylammonium salts. [c] Determined by the UV-vis titration experiments in CH_3CN, due to the inability to measure K_a value accurately by ^{1}H NMR titration method. [d] NB = no binding.

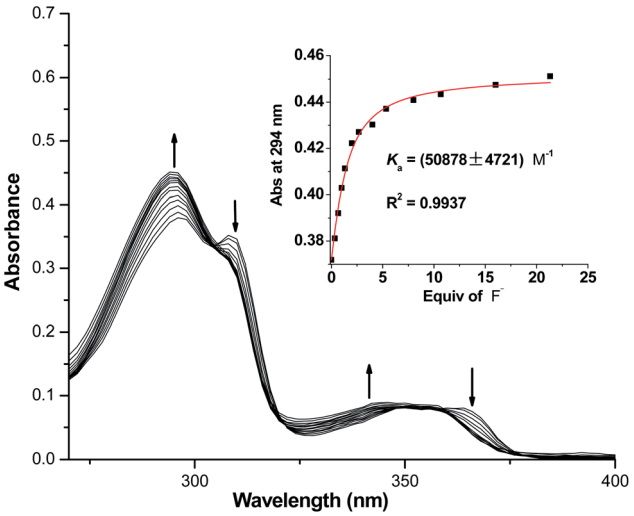

Fig. 4 UV-vis titration of macrocycle **1** (20 μM) with TBAF in CH_3CN (Inset: A 1 : 1 non-linear curve fitting of the absorbance at 294 nm of macrocycle **1** against the added F^-).

anions, the affinity of **2** for HSO_4^- was most significantly enhanced (with respect to **1**), which may result from the existence of an additional hydrogen bond between bisulfate hydroxyl proton and pyridine nitrogen atom of **2**.[27]

It should be noted that macrocycle **1** displayed a remarkable improvement in the binding selectivity for fluoride over chloride, acetate, benzoate, and dihydrogenphosphate anions (relative to macrocycle **2**), as revealed by selectivity factors expressed as ratios of the related binding constants $K_a(F^-)/K_a(Cl^-)$, $K_a(F^-)/K_a(CH_3COO^-)$, $K_a(F^-)/K_a(PhCOO^-)$, and $K_a(F^-)/K_a(H_2PO_4^-)$. For example, a 5.3-fold preference for F^- over $H_2PO_4^-$ in **2** was improved moderately to 10.3-fold in the case of **1**. Moreover, the binding selectivity of **1** for F^- over $PhCOO^-$ was pronouncedly improved from 6.4 (in the case of **2**) to 50.2. In addition, a 13.7 : 1 selectivity for F^- over CH_3COO^- in **2** was increased sharply to 182.4 : 1 as for **1**. More significantly, the binding selectivity for F^- over Cl^- was dramatically enhanced from 38.6 to 559.1, while changing the macrocycles from **2** to **1**. In a word, a slight structural change in these macrocyclic receptors gave rise to profound influences not only on the binding affinity but also on the binding selectivity.

Previous studies have documented that solvent effects in supramolecular systems played a significant role in the affinity and selectivity of anion receptors.[28–30] Thus, we subsequently studied recognition properties of **1** in the more polar DMSO-d_6 medium. As displayed in Fig. 5a, the addition of 0.2 equiv. of F^- firstly triggered a significant broadening of the signals assigned to carbazole NH and sulfonamide NHs, and then they experienced a thorough disappearance while continually increasing the concentration of fluoride ion. Meanwhile, the resonance of aromatic CH proton was found to progressively move downfield from 7.17 to 7.59 ppm. Noteworthily, no NH deprotonation event took place for **1** before the addition of 2.8 equiv. of F^-. In other words, a small amount of F^- firstly formed hydrogen-bonded complex with **1**, and then more F^- (≥2.8 equiv.) induced NH deprotonation in **1** (as evidenced by the appearance of a characteristic triplet of the HF_2^- species centered at 16.20 ppm).[31,32] Based on the titration data extracted from hydrogen-bonding interaction stage, a rough K_a of 147 M^{-1} (Fig. 5b) was determined (a 1 : 1 binding stoichiometry between **1** and F^- in DMSO-d_6 supported by Job plot method in Fig. S21†). Interestingly, upon addition of other competitive anions like $H_2PO_4^-$ and CH_3COO^- (Fig. S13 and S15†), only the disappearance of two NH signals was observed for **1** (probably due to a rapid proton exchange process),[33] without meaningful chemical shift changes for other proton signals. These observations demonstrated no or very weak binding of **1** with these anions in this medium.[34,35] Taken together, macrocycle **1** achieved an exclusive recognition towards fluoride ion in the strongly polar DMSO-d_6 medium, albeit with a moderate affinity.

Single crystals of fluoride complex of macrocycle **1** were obtained by slow evaporation of an acetonitrile solution of **1** in the presence of excess fluoride ion. Unexpectedly, the binding model in the solid state (**1**/F^- = 2 : 1) turned out to be different from that observed in solution (**1**/F^- = 1 : 1). As seen from Fig. 6, one fluoride ion was captured by two sulfonamide NH groups (N···F distances of 2.650 and 2.641 Å, respectively, and the corresponding N–H···F angles of 160.4 and 169.1°) from two adjacent host molecules. This disparity in the binding stoichiometry between solution phase and solid state had been previously reported,[36–40] likely resulting from molecular packing effect in the latter case.[37]

In order to shed more light on the nature of the formed complex between macrocycle **1** and fluoride ion, density functional theory (DFT) calculations were performed at the B3LYP/6-311++G(d,p) level under the polarizable continuum model

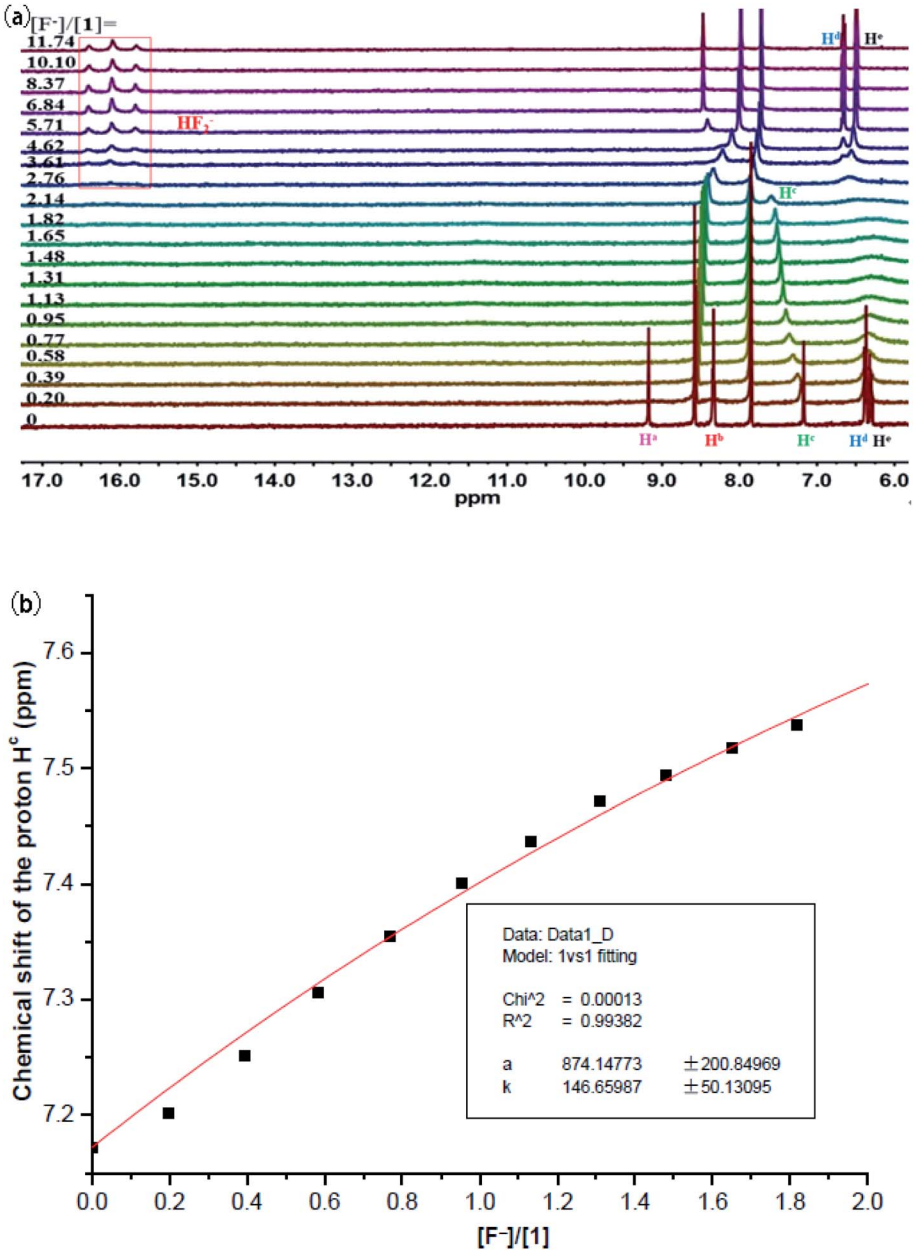

Fig. 5 (a) ^{1}H NMR titration of macrocycle **1** (1.6 mM) with TBAF in DMSO-d_6. (b) Fitting binding isotherms of macrocycle **1** with TBAF in DMSO-d_6 at 298 K, showing chemical shift changes of the proton H^c based on a 1 : 1 binding model.

(PCM) using CH_3CN as a solvent in the Gaussian 16 package. As shown in Fig. 7, an energy-minimized structure of the 1 : 1 **1**/F^- complex confirmed the presence of four intermolecular hydrogen bonds involving **1** and the bound F^- ion. More specifically, the F⋯N/C distances between F^- and four hydrogen-bond donors (one carbazole NH, two sulfonamide NHs and one aromatic CH units) were determined to be 2.567, 2.768, 2.814, and 2.964 Å, respectively. Combined with their bond angles (172.74, 171.68, 167.28, and 90.41°, respectively), a conclusion could be drawn that carbazole NH and sulfonamide NHs made a main contribution to the stabilization of the **1**/F^- complex. In the meanwhile, aromatic CH group from the 1,3-xylyl linker also played a role in the hydrogen-bonding interaction with fluoride, albeit a relatively smaller contribution. These results of molecular optimization were in good agreement with the aforementioned ^{1}H NMR titration experiments in CD_3CN (Fig. 2). Of note, macrocycle **1** had to undergo a conformational change (from a divergent pattern to a convergent style as for the NH/CH binding units) for cooperative utilization of four hydrogen-bond donors for the fluoride binding. Interestingly, the dihedral angle between carbazole plane and phenyl ring remained nearly unchanged (12.21° in the resulting complex), that is, a near 180-degree rotation took place for the benzene ring of **1** upon fluoride binding.

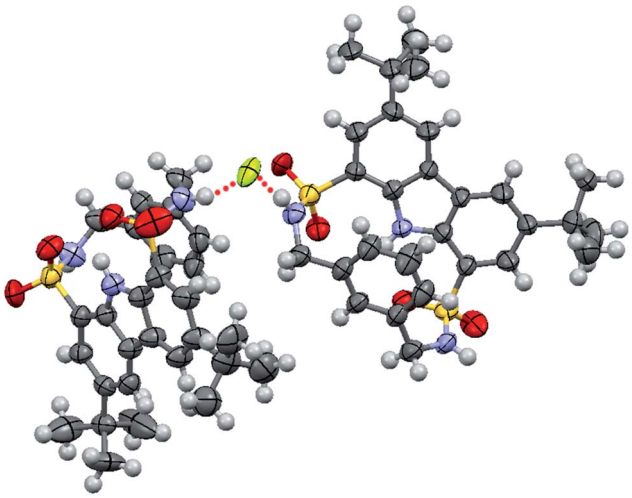

Fig. 6 Crystal structure of the formed complex between macrocycle **1** and fluoride ion. The counterion (TBA^+) was omitted for clarity.

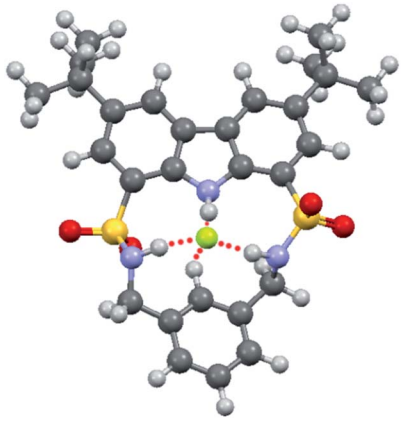

Fig. 7 DFT-optimized structure of macrocycle **1**/F^- complex.

Conclusions

In summary, two carbazole sulfonamide-based macrocycles **1** and **2** were facilely prepared and assessed as anion receptors by ^{1}H NMR, UV-vis titration, solid-state X-ray, and DFT calculation methods. The obtained results indicated that macrocycle **1** had a powerful and selective binding towards fluoride ion in acetonitrile solution, over its strong competitors including CH_3COO^- and $H_2PO_4^-$ anions. More importantly, macrocycle **1** was found to recognize F^- exclusively in the more polar DMSO-d_6 solution. As a well-performed anion receptor, macrocycle **1** may have the potential for future applications in fluoride sensing, transmembrane fluoride transport and fluoride extraction, after a further structural modification.

Experimental

Materials and general methods

All the chemicals were purchased from commercial suppliers and used without further purification (unless stated otherwise). Melting points were measured on a XT-4 binocular microscope (Beijing Tech Instrument Co., China) and uncorrected. All the ^{1}H and ^{13}C NMR data were determined on a JEOL-ECX 500 NMR spectrometer at 298 K using TMS as an internal standard, and chemical shift (δ) was expressed in parts per million (ppm). The following abbreviations were utilized in expressing the multiplicity: s = singlet, d = doublet, t = triplet, q = quartet, m = multiplet. High resolution mass spectra (HRMS) were recorded on a Thermo Scientific Q Exactive Hybrid Quadrupole-Orbitrap mass spectrometer. UV-vis spectra were collected on a Beijing PGENERAL TU-1900 spectrometer. The X-ray crystallographic data were collected using a Bruker D8 Venture diffractometer. All the non-linear curve fitting analysis were conducted using the previously-reported equations[41] and the software of Origin 6.0.

Synthesis

Synthesis of macrocycle 1. A solution of carbazole-1,8-disulfonyl chloride **3** (118 mg, 0.25 mmol) in dry CH_2Cl_2 (20 mL) was added dropwise into a dry CH_2Cl_2 solution (20 mL) containing 1,3-xylylenediamine (33 μL, 0.25 mmol) and TEA (0.2 mL) over 0.5 h. After the addition was completed, the reaction mixture was continuously stirred for 3 h at room temperature. The solvent was then evaporated under reduced pressure, and the obtained residue was subjected to column chromatography separation on silica gel using petroleum ether–ethyl acetate (5 : 1, *v*/*v*) as an eluent, yielding **1** as a white solid (40.4 mg, 30% yield), mp > 250 °C. ^{1}H NMR (500 MHz, CD_3CN) δ: 9.14 (s, 1H), 8.44 (d, J = 5.0 Hz, 2H), 7.91 (d, J = 5.0 Hz, 2H), 7.14 (s, 1H), 6.52 (d, J = 5.0 Hz, 2H), 6.34–6.30 (m, 3H), 4.18 (d, J = 5.0 Hz, 4H), 1.47 (s, 18H); ^{1}H NMR (500 MHz, DMSO-d_6) δ: 9.18 (s, 1H), 8.58 (d, J = 5.0 Hz, 2H), 8.34 (t, J = 5.0 Hz, 2H), 7.86 (d, J = 5.0 Hz, 2H), 7.17 (s, 1H), 6.38 (d, J = 5.0 Hz, 2H), 6.31–6.28 (m, 1H), 4.07 (d, J = 5.0 Hz, 4H), 1.45 (s, 18H); ^{13}C NMR (125 MHz, DMSO-d_6) δ: 142.4, 136.7, 133.4, 130.6, 127.0, 126.4, 123.5, 122.8, 122.4, 122.3, 46.3, 34.7, 31.6; HRMS (ESI) *m*/*z*: $[M + H]^+$ calcd for $C_{28}H_{34}N_3O_4S_2$: 540.1985, found: 540.1978.

Synthesis of macrocycle 2. Macrocycle **2** was synthesized in a similar manner to macrocycle **1**, except for the use of 2,6-lutidinylenediamine instead of 1,3-xylenediamine as the starting material. 25% yield, mp > 250 °C. ^{1}H NMR (500 MHz, CD_3CN) δ: 9.47 (s, 1H), 8.41 (d, J = 5.0 Hz, 2H), 8.01 (d, J = 5.0 Hz, 2H), 7.01–6.98 (m, 3H), 6.46 (d, J = 10.0 Hz, 2H), 4.07 (d, J = 10.0 Hz, 4H), 1.47 (s, 18H); ^{1}H NMR (500 MHz, DMSO-d_6) δ: 10.50 (s, 1H), 9.09 (t, J = 5.0 Hz, 2H), 8.53 (d, J = 5.0 Hz, 2H), 7.96 (d, J = 5.0 Hz, 2H), 6.91 (t, J = 10.0 Hz, 1H), 6.34 (d, J = 10.0 Hz, 2H), 4.06 (d, J = 5.0 Hz, 4H), 1.43 (s, 18H); ^{13}C NMR (125 MHz, DMSO-d_6) δ: 155.1, 142.8, 136.5, 133.1, 124.9, 124.6, 122.9, 121.2, 120.1, 46.9, 35.1, 32.0; HRMS (ESI) *m*/*z*: $[M + H]^+$ calcd for $C_{27}H_{33}N_4O_4S_2$: 541.1938, found: 541.1951.

^{1}H NMR titration studies

^{1}H NMR titrations were performed on a JEOL-ECX 500 NMR spectrometer, working at a frequency of 500 MHz with the probe temperature at 298 K. All the tested anions were added as their tetra-*n*-butylammonium (TBA) salts. In all cases, the ^{1}H NMR

titrations were carried out while keeping the concentration of the macrocycles **1** or **2** (1.6 mM in CD_3CN or DMSO-d_6) constant through dissolving guest anions with the same macrocycle solution to prepare guest solution. The guest solution was then progressively added to the macrocycle solution using an appropriate pipette, and the resulting ^{1}H NMR spectrum was recorded after each addition. The above operations ensured that the concentration of the macrocycle remained constant, whilst the concentration of the added anions varied. Finally, a non-linear curve fitting analysis using a 1 : 1 binding model was performed to fit experimental data and gave the corresponding binding constants (K_a).[41]

UV-vis titration studies

UV-vis titration studies were conducted on a TU-1900 UV-visible spectrophotometer, by adding an acetonitrile solution containing guest anions F^- or OH^- (20 mM, using their tetrabutylammonium salts) into an acetonitrile solution of the macrocycle (20 μM) in a quartz cuvette at 298 K. The resultant UV-vis spectra were recorded after each addition. Finally, the absorbance values at the specific wavelength were plotted against equivalents of the added anions and fitted based on a 1 : 1 binding stoichiometry.[41]

Conflicts of interest

There are no conflicts to declare.

Acknowledgements

We gratefully thank the National Natural Science Foundation of China (No. 21161005) for financial support.

Notes and references

1 Y. Zhou, J. F. Zhang and J. Yoon, *Chem. Rev.*, 2014, **114**, 5511–5571.
2 M. Cametti and K. Rissanen, *Chem. Soc. Rev.*, 2013, **42**, 2016–2038.
3 M. Cametti and K. Rissanen, *Chem. Commun.*, 2009, 2809–2829.
4 M. Vázquez, L. Fabbrizzi, A. Taglietti, R. M. Pedrido, A. M. González-Noya and M. R. Bermejo, *Angew. Chem., Int. Ed.*, 2004, **43**, 1962–1965.
5 K. J. Chang, D. Moon, M. S. Lah and K. S. Jeong, *Angew. Chem., Int. Ed.*, 2005, **44**, 7926–7929.
6 S. O. Kang, J. M. Llinares, D. Powell, D. VanderVelde and K. Bowman-James, *J. Am. Chem. Soc.*, 2003, **125**, 10152–10153.
7 R. Nishiyabu and P. Anzenbacher, *J. Am. Chem. Soc.*, 2005, **127**, 8270–8271.
8 R. Nishiyabu, M. A. Palacios, W. Dehaen and P. Anzenbacher, *J. Am. Chem. Soc.*, 2006, **128**, 11496–11504.
9 R. Nishiyabu and P. Anzenbacher, *Org. Lett.*, 2006, **8**, 359–362.
10 G. W. Bates, P. A. Gale and M. E. Light, *Chem. Commun.*, 2007, 2121–2123.
11 J. Yoo, M. S. Kim, S. J. Hong, J. L. Sessler and C. H. Lee, *J. Org. Chem.*, 2009, **74**, 1065–1069.
12 R. Samanta, B. S. Kumar and P. K. Panda, *Org. Lett.*, 2015, **17**, 4140–4143.
13 P. A. Gale, *Chem. Commun.*, 2008, 4525–4540.
14 K. Choi and A. D. Hamilton, *Coord. Chem. Rev.*, 2003, **240**, 101–110.
15 M. Chmielewski and J. Jurczak, *Tetrahedron Lett.*, 2004, **45**, 6007–6010.
16 C. Caltagirone, G. W. Bates, P. A. Gale and M. E. Light, *Chem. Commun.*, 2008, 61–63.
17 D. Mondal, A. Sathyan, S. V. Shinde, K. K. Mishra and P. Talukdar, *Org. Biomol. Chem.*, 2018, **16**, 8690–8694.
18 Y. C. He, Y. M. Yan, H. B. Tong, Z. X. Ren, J. H. Wang, Y. B. Zhang, J. B. Chao and M. L. Wang, *Chem. Commun.*, 2020, **56**, 9364–9367.
19 Y. Hua and A. H. Flood, *Chem. Soc. Rev.*, 2010, **39**, 1262–1271.
20 Z. Li, C. Rao, L. Chen, C. Fu, T. Zhu, X. Chen and C. Liu, *J. Org. Chem.*, 2019, **84**, 7518–7522.
21 L. M. Eytel, H. A. Fargher, M. M. Haley and D. W. Johnson, *Chem. Commun.*, 2019, **55**, 5195–5206.
22 F. Zhang, Y. H. Zhou and X. P. Bao, *Supramol. Chem.*, 2016, **28**, 305–313.
23 Á. L. Fuentes de Arriba, M. G. Turiel, L. Simón, F. Sanz, J. F. Boyero, F. M. Muñiz, J. R. Morán and V. Alcázar, *Org. Biomol. Chem.*, 2011, **9**, 8321–8327.
24 X. P. Bao, X. Wu, S. N. Berry, E. N. W. Howe, Y. T. Chang and P. A. Gale, *Chem. Commun.*, 2018, **54**, 1363–1366.
25 N. Busschaert, M. Wenzel, M. E. Light, P. Iglesias-Hernández, R. Pérez-Tomás and P. A. Gale, *J. Am. Chem. Soc.*, 2011, **133**, 14136–14148.
26 V. Mazzini and V. S. J. Craig, *Chem. Sci.*, 2017, **8**, 7052–7065.
27 M. J. Chmielewski and J. Jurczak, *Tetrahedron Lett.*, 2005, **46**, 3085–3088.
28 C. Caltagirone, J. R. Hiscock, M. B. Hursthouse, M. E. Light and P. A. Gale, *Chem.–Eur. J.*, 2008, **14**, 10236–10243.
29 C. Caltagirone, P. A. Gale, J. R. Hiscock, S. J. Brooks, M. B. Hursthouse and M. E. Light, *Chem. Commun.*, 2008, 3007–3009.
30 X. P. Bao, Y. H. Zhou and B. A. Song, *Sens. Actuators, B*, 2012, **171–172**, 550–555.
31 L. T. Wang, X. M. He, Y. Guo, J. Xu and S. J. Shao, *Org. Biomol. Chem.*, 2011, **9**, 752–757.
32 S. O. Kang, D. Powell, V. W. Day and K. Bowman-James, *Angew. Chem., Int. Ed.*, 2006, **45**, 1921–1925.
33 Z. A. Tabasi, E. A. Younes, J. C. Walsh, D. W. Thompson, G. J. Bodwell and Y. M. Zhao, *ACS Omega*, 2018, **3**, 16387–16397.
34 S. J. Choi, B. Yoon, J. D. Ray, A. Netchaev, L. C. Moores and T. M. Swager, *Adv. Funct. Mater.*, 2020, **30**, 1907087.
35 G. Picci, M. Kubicki, A. Garau, V. Lippolis, R. Mocci, A. Porcheddu, R. Quesada, P. C. Ricci, M. A. Scorciapino and C. Caltagirone, *Chem. Commun.*, 2020, **56**, 11066–11069.
36 M. D. Gu, Y. Lu and M. X. Wang, *J. Org. Chem.*, 2020, **85**, 2312–2320.

37 S. Sugiura, Y. Kobayashi, N. Yasuda and H. Maeda, *Chem. Commun.*, 2019, **55**, 8242–8245.
38 S. Xiong, F. Chen, T. Zhao, A. Li, G. Xu, J. L. Sessler and Q. He, *Org. Lett.*, 2020, **22**, 4451–4455.
39 C. J. Serpell, A. Y. Park, C. V. Robinson and P. D. Beer, *Chem. Commun.*, 2021, **57**, 101–104.
40 C. Guo, H. Wang, V. M. Lynch, X. Ji, Z. A. Page and J. L. Sessler, *Chem. Sci.*, 2020, **11**, 5650–5657.
41 P. Thordarson, *Chem. Soc. Rev.*, 2011, **40**, 1305–1323.